J Bioenerg Biomembr (2011) 43:275–285
DOI 10.1007/s10863-011-9350-y

Online monitoring of metabolism and morphology of peptide-treated neuroblastoma cancer cells and keratinocytes

Sabine Drechsler · Jörg Andrä

Received: 9 November 2010 / Accepted: 27 March 2011 / Published online: 4 June 2011

Abstract Antimicrobial peptides are promising anti-cancer agents with a unique mode of action. We established the usage of a chip-based sensor to monitor the dynamic interplay between cells on the chip and peptides and compared it with endpoint tests. Human neuroblastoma cancer cells and spontaneously immortalized non-cancer keratinocytes were perfused with representative peptides (NK-2, NK11, and melittin). The sensor system enabled continuous recording of cell layer impedance (adhesion/confluence), oxygen consumption (respiration) and extracellular acidification (glycolysis) and provided insights in cell damage, stress response and recovery. Cells responded differentially to peptide treatment. During perfusion, peptides accumulated on the cell surface until they reached a critical concentration. Preceding to cell death, melittin triggered glycolysis, suggesting stress response. NK-2 induced no change in energy metabolism, but led to an increase in impedance, i.e. a temporarily altered morphology, which appeared to be an excellent parameter to detect subtle structural changes of cell layers.

Keywords Antimicrobial peptide · Biosensor · Cancer · Glycolysis · HaCaT · Impedance · Keratinocytes · Membrane permeabilization · Neuroblastoma · Respiration

J. Andrä (✉)
Division of Biophysics, Research Center Borstel,
Leibniz-Center for Medicine and Biosciences,
Parkallee 10,
23845 Borstel, Germany
e-mail: jandrae@fz-borstel.de

S. Drechsler
Bionas GmbH,
Rostock, Germany

Abbreviations

AMP	antimicrobial peptide
BRM	bionas running medium
LDH	lactate dehydrogenase
NBD	N-(7-nitrobenz-2-oxa-1,3-diazol-4yl)
MTT	3-[4,5-dimethylthiazol-2-yl]-2,5-diphenyltetrazolium bromide
NB	neuroblastoma
PI	propidium iodide

Introduction

Most of the commonly used chemotherapeutics for the treatment of cancer are also harmful to healthy human cells. Consequently, patients undergoing chemotherapy usually suffer from detrimental side effects (Stortecky and Suter 2010). Furthermore, cancer cells develop multi-drug resistance (MDR) proteins to expel the drugs from the cell (Andjelkovic et al. 2008). As a promising alternative, so-called antimicrobial peptides (AMPs) have been emerged as anti-cancer agents ((Baker et al. 1993; Bodek et al. 2005; Cruciani et al. 1991; Makovitzki et al. 2009; Papo et al. 2006; Warren et al. 2001), for recent reviews see (Hoskin and Ramamoorthy 2008; Schweizer 2009)).

AMPs, also termed host defense peptides, are widespread in nature (Jenssen et al. 2006; Zasloff 2002). They are gene-encoded peptides, which normally provide a first line of defence against invading microbes on epithelial tissues and are part of the armament of professional immune cells. Examples are frog magainins (Zasloff 1987), cathelicidins (Larrick et al. 1995; Zanetti et al. 1995) and the human β–defensins (Harder et al. 1997; Harder et al. 2001). In contrast to common antibiotics, most

AMPs interact not specifically with a bacterial enzyme or protein receptor, but directly with the lipid matrix of their targets. This is achieved by an amphipathic secondary structure of AMPs resulting in the segregation of hydrophobic and cationic surface areas of these molecules. Interaction of AMPs with target cell membranes eventually leads to the formation of lesions or pores and with that to a disturbance or destruction of membrane potential and of the membrane barrier function (Bechinger and Lohner 2006). Killing by this mechanism is rapid and aggravates the emergence of strains, which are resistant to these peptides. Most AMPs target specifically bacteria and are almost non-toxic for host cells. This differential sensitivity is driven by electrostatic interactions with the negatively charged lipids of the bacterial membranes (Hammer et al. 2010; Matsuzaki et al. 1995; Schröder-Borm et al. 2003). Interestingly, it has been shown that some cancer cells are killed by certain AMPs, whereas primary cells, such as blood lymphocytes, endothelial cells and fibroblasts were not affected by the peptides (Chen et al. 2010; Cruciani et al. 1991; Hui et al. 2002; Johnstone et al. 2000; Schröder-Borm et al. 2005; Tang et al. 2010).

There are several important advantages which endorse the application of AMPs as anti-cancer drugs. Due to their unique mode of action, they exhibit broad spectrum activity and are generally not affected by resistance mechanism to commonly used drugs (Johnstone et al. 2000; Kim et al. 2003; Wang et al. 2009). They can be easily added to a conventional therapy and then act in synergy with chemotherapeutics and overcome resistance mechanism (Chuang et al. 2008; Ohsaki et al. 1992; Papo et al. 2004). Moreover, it may be speculated that they prevent growth of metastases if given systemically and, as they are potent antimicrobials, AMPs are likely to protect from bacterial infections during or after surgery.

Up to now, the toxicity of peptides against cancer cells has been documented in vitro using classical endpoint tests. Cytotoxicity endpoint tests, such as the metabolic MTT test or assays to detect the release (LDH) or uptake (PI) of marker proteins and dyes, respectively, are suitable for peptide screening and to give a first impression whether membrane effects are involved in the peptides activities (LDH and PI assay). As a disadvantage, they provide no insights into the dynamics of the interplay between peptides and cells. Since they are normally evaluated after a certain time point (endpoint), they will overlook kinetics as well as cell damages, which occur at an early time point and which are repaired by the cells during incubation time. To close this gap in the understanding of the mode of action of AMPs as anti-cancer agents, we utilized a chip-based analyzing system, which allows the continuous and label free determination of cell metabolism and cell morphology over time (Abarzua et al. 2010; Ceriotti et al. 2007; Thedinga et al. 2007). Cells were grown on a chip surface, which is equipped with pH, oxygen and impedance sensors. Peptides diluted in medium are applied to the cells at a defined flow rate. At regular time points, the flow is stopped for a couple of minutes and the consumption of oxygen, the change in pH, and the impedance of the cell layer were simultaneously measured. Extracellular pH and pO_2 are mainly influenced by cellular glycolysis and respiration, respectively. Both are measures of cell metabolism. The impedance of the cell layer is influenced by the density and adhesion of the cell layer, the shape of the cells and the contact zone between the cells and, hence, is a sensitive measure of morphological changes within single cells and the cell layer (Thedinga et al. 2007).

Using this chip-based sensor system, we investigated the interactions of two representative AMPs and one inactive variant thereof (Table 1) with two established human cell lines. The peptides, i.e. melittin from bee venom (Dempsey 1990; Habermann and Jentsch 1967) and NK-2 (Andrä and Leippe 1999), an internal fragment of porcine NK-lysin, are well-characterized and exhibit pronounced antimicrobial and anti-cancer cell activities (Andrä et al. 2007; Russell et al. 2004; Schröder-Borm et al. 2005). Though NK-2 and melittin are both cationic as well as similar in size and structure, they are characterized by different degrees of target selectivity and hydrophobicity. As target cells we used the neuroblastoma cancer cell line LA-N-1 (Schröder-Borm et al. 2005) and the spontaneously immortalized non-cancer keratinocyte cell line HaCaT (Boukamp et al. 1988). LA-N-1 and HaCaT cells were of high and low sensitivity to the action of the peptide NK-2, respectively (Andrä and Leippe 1999; Schröder-Borm et al. 2005). Moreover, we determined the hemolytic activity of peptides, the binding of fluorescently-labelled peptides to the cells and compared the biosensor data with classical endpoint tests for cytotoxicity. To our knowledge, this is the first report, in which the dynamic interplay of membrane-interacting peptides and cancer cells in terms of cellular metabolism and morphology/adhesion has been comprehensively monitored.

Materials and methods

Peptides

Peptides were synthesized with an amidated C terminus by the Fmoc solid-phase peptide synthesis technique on an automatic peptide synthesizer (model 433 A; Applied Biosystems) as described (Andrä et al. 2004). NBD-labelled peptides were prepared as follows: Peptide coupled to the resin and with protected side chains was suspended in dimethylformamide, supplemented with trace amounts of

Table 1 Amino acid sequence, net charge, hydrophobicity (GRAVY, grand average of hydropathy) of synthetic peptides used in this study

Peptide	Source	Sequence	Net charge	GRAVY
NK-2	Pig	KILRG VCKKI MRTFL RRISK DILTG KK	+10	−0.263
NK11	(NK-2)	KISKR ILTGK K	+6	−0.836
Melittin	Honey bee	GIGAV LKVLT TGLPA LISWI KRKRQ Q	+6	+0.273

pyridine. Then, a 4-fold molar excess of 4-chloro-7-nitro-1,2,3-benzoxadiazole (NBD chloride, Fluka, Germany) was added and the suspension was stirred gently overnight at 20 °C. The resin was filtered, washed and the peptide was cleaved from the resin as described above. Purified and lyophilized peptides were diluted 1 mM in 0.01% TFA and stored at −20 °C until use.

Calculation of hydrophobicity values of peptides

All calculations were done using the Expasy proteomics server (http://expasy.org). The GRAVY (Grand Average of Hydropathy) value for a peptide or protein was calculated as the sum of hydropathy values (Kyte and Doolittle 1982) of all the amino acids, divided by the number of residues in the sequence. Hydrophobicity plot was generated using the consensus scale proposed by Eisenberg (Eisenberg et al. 1984) and a window size of 7.

Assay for hemolytic activity

Freshly isolated and washed human erythrocytes (5×10^8 cells/ml) in 20 µl PBS, pH 7.4, were incubated with 80 µl of a peptide sample in the same buffer for 30 min at 37 °C in a round bottom 96-well plate (Nunclon Surface, Nunc, Roskilde, Denmark). After the incubation period the plate was centrifuged at 1000×g for 10 min to remove intact erythrocytes, and the concentration of released hemoglobin was measured in a microtiter plate reader at 405 nm (Rainbow, Tecan, Grödig/Salzburg, Austria) after ten-fold dilution of the supernatant. Hemolytic activity was expressed as percent hemolysis (% hemolysis=((OD_{Sample}-OD_{buffer})/(OD_{max}-OD_{buffer})*100). Maximal lysis (OD_{max}) was achieved by adding distilled water instead of the peptide sample to the cells. Data shown represent the mean of at least two experiments each performed in duplicate.

Culture and harvesting of human cell lines

Human cells used in this study were the keratinocyte cell line HaCaT (Boukamp et al., 1988), and the neuroblastoma cell line LA-N-1 (Schröder-Borm et al. 2005). Cells were cultured in very low endotoxin (VLE)-RPMI 1640 (LA-N-1) or DMEM (HaCaT), each supplemented with 10% heat-inactivated FCS, L–glutamine, penicillin and streptomycin at 37 °C in a humidified atmosphere at 5% CO_2. Both media were supplied from Biochrom (Berlin, Germany). Cells were harvested by addition of 1 ml of trypsin/EDTA in PBS (Biochrom) and incubation at 37 °C.

Preparation of 96-well plates for MTT and LDH assays

Freshly harvested cells were suspended in cell culture medium with 10% FCS to a density of 2.5×10^5 cells/ml. This suspension (100 µl) was filled in each well of a sterile flat-bottom 96-well microtiter plate (Costar tissue culture treated, Corning Incorporated, NY, USA). After incubation at 37 °C in a humidified atmosphere with 5% CO_2 for 24 h, the medium was removed.

MTT assay

Metabolic activity, i.e. viability, of cells was determined in 96-well plates using the TOX-1 kit following the instructions of the manufacturer (SigmaAldrich, Steinheim, Germany). Peptides, diluted from stock solutions in 0.01% TFA into a mixture (v/v) of 10% standard cell culture medium and 90% PBS, pH 7.4, were added to the wells (100 µl each) of a 96-well plate to initially seeded 25.000 cells and were incubated for 4 h at 37 °C. As controls, medium/PBS (M_{PBS}=100% viability) and 5% triton X-100 in PBS (M_T=0% viability) were added to wells loaded with cells. For determination of cell viability, 10 µl of a solution (5 mg/ml) of the tetrazolium salt 3-[4,5-dimethylthiazol-2-yl]-2,5-diphenyltetrazolium bromide (MTT) in PBS, pH 7.4, was added to each well and incubated for 2 h at 37 °C. Formed formazan crystals were dissolved by adding 10% triton in acid isopropanol (100 µl) to each well, and the extinction was measured using a microtiter-plate reader at absorbance and reference wavelenghts of 570 and 690 nm, respectively. Each experiment was performed in duplicates and performed at least twice. Metabolic activity (%M) of the cells was calculated using the following equation: $\%M = 100 \times \left((M_{Exp} - M_T)/(M_{PBS} - M_T)\right)$.

LDH assay

Peptide-induced lysis of adherent cells was determined in 96-well plates using the Cytotoxicity Detection Kit based on the release of lactate dehydrogenase (LDH) from lysed cells following the instructions of the manufacturer (Roche, Mannheim, Germany). Peptides, diluted from stock sol-

utions in 0.01% TFA into PBS, pH 7.4 or in Bionas running medium (BRM, pH 7.4, see below), were added to the wells (200 µl each) to initially seeded 25.000 cells and were incubated for 4 h at 37 °C. As controls, PBS or BRM ($L_{control}$=0% lysis) and 5% triton X-100 in PBS or BRM (L_T=100% lysis) were added to wells loaded with cells. After incubation, the plate was centrifuged and 100 µl of the supernatants were transferred into another 96-well plate. LDH reaction mixture (100 µl) was added, incubated in the dark for 5 min at room temperature. The reaction was stopped by adding 50 µl stop solution. Finally, the extinction was measured using a microtiter-plate reader at absorbance and reference wavelenghts of 490 nm and 630 nm, respectively. Each experiment was performed in duplicates and repeated at least once. Cell lysis (%L) was calculated using the following equation: $\%L = 100\times \left(\left(L_{Exp} - L_{control}\right)/\left(L_T - L_{control}\right)\right)$.

PI-uptake assay

Suspended cells with compromized membranes were detected by monitoring the uptake of the DNA-intercalating dye propidium iodide (PI) into the cells. Freshly harvested cells (see above) were washed twice with PBS, pH 7.4, and sedimented. Peptides (100 µl) diluted in PBS were added to the cell pellet (2×10^5), the cells were gently vortexed and incubated with the peptides for 30 min at 37 °C. Then, PI (5 µl, 100 µg/ml, Invitrogen, Eugene, Oregon, USA) was added and the suspension was further incubated for 5 min at 4 °C in the dark. The reaction mixtures were diluted in ice-cold buffer and analyzed with a FACSCalibur (Becton Dickinson, Heidelberg, Germany) flow cytometer with computer-assisted evaluation of data (CellQuest software). Cell lysis (%L) was calculated from the percentage of PI positive cells in buffer alone ($PI_{control}$) and in the presence of peptides (PI_{exp}): $\%L = 100\times \left(\left(PI_{exp} - PI_{control}\right)/\left(100 - PI_{control}\right)\right)$.

Binding of NBD-labelled peptides to cells

Freshly harvested cells (see above) were washed twice with PBS, pH 7.4, and sedimented. NBD-labelled Peptides (100 µl) diluted in PBS were added to the cell pellet (2×10^5), the cells were gently vortexed and incubated with the peptides for 30 min at 37 °C. These mixtures were diluted in ice-cold buffer and analyzed with a FACSCalibur (Becton Dickinson, Heidelberg, Germany) flow cytometer with computer-assisted evaluation of data (CellQuest software).

Online monitoring of cell metabolism

For the online monitoring of three important cell physiological parameters we used the Bionas analyzing system 1500^2 and 2500 (Bionas GmbH, Rostock, Germany). Cells were grown adherently on a metabolic biosensor chip (SC1000, Bionas) equipped with clark, ISFET, and IDES sensors, which allow the simultaneous determination of oxygen consumption, extracellular acidification and cell impedance, respectively. Before each experiment the tube system was disinfected with 70% ethanol and then rinsed with PBS and conditioned with Bionas running medium (BRM). BRM is a cell culture medium without bicarbonate buffer but with 1 mM Hepes, pH 7.4, 4.5 g/l glucose, 0.1% FCS, 100 U/ml penicillin and 100 µg/ml streptomycin (Bionas GmbH, Rostock, Germany). Chips were also disinfected with 70% ethanol, rinsed with PBS and then conditioned with the respective standard cell culture medium. Freshly harvested cells (2×10^5) were seeded on the chips and cultivated in the respective standard medium for 24 h at 37 °C and 5% CO_2 in a humidified atmosphere. After mounting the chips in the biomodules of the Bionas system they were flushed with BRM. The system was operated with low buffered running medium to allow the assessment of changes in pH at a flow rate of 56 µl/min with alternating "go" and "stop" phases of 4 min each. During the "go" phase, cells on the chip are perfused with fresh medium or medium with compound. In the subsequent "stop" phase, oxygen consumption and extracellular acidification in the cell supernatant of each chip were measured continuously. The change of the parameter, i.e. the rate, is calculated for each "stop" phase and represents the metabolic activity of the cells and is given as a single data point in the figures. Cell impedance was monitored during the whole run independently of the pump state and its mean value is given as a single data point. One chip with cells served as a control and was fed with running medium without test compounds. Data are presented normalized to untreated control cells in medium. Finally, the biomodules were rinsed with 0.2% triton X-100 in BRM to achieve complete cell lysis.

Results

Hydrophobicity analyses of peptides

The analysis of the hydrophobicity profiles of the peptides revealed pronounced differences despite that they are all of a similar length, charge and secondary structure (Fig. 1). The profile of NK-2 is characterized by alternating hydrophilic and hydrophobic amino acid residues reflecting the turns of an α-helix, which indicates a highly amphipathic structure. Melittin exhibited a completely different profile. The sequence of this peptide is divided into a hydrophobic part and a C-terminal hydrophilic part. In average, NK-2 appears hydrophilic and melittin hydrophobic (Table 1).

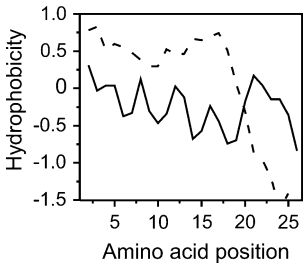

Fig. 1 Hydrophobicity plots of peptides. Hydrophobicity values were calculated using the Eisenberg scale for hydrophobicity (Eisenberg et al. 1984). NK-2, solid black; melittin, dashed black curve

Hemolytic activity of peptides

The hemolytic activity of peptides against freshly isolated human erythrocytes was determined photometrically by monitoring the release of hemoglobin (Fig. 2). The activity correlated with the average hydrophobicity of the peptides (Table 1): Melittin exhibited strong activity, NK-2 was moderately hemolytic and NK11 was complete inactive.

Cytotoxicity tests

The direct toxicity of peptides against LA-N-1 and HaCaT cells was analyzed by the use of three established assays (Table 2):

i) The effect of the peptides on the metabolic activity of cells was determined by the MTT assay (Fig. 3). By this assay, the conversion of a tetrazolium salt (MTT) into formazan by adherently growing cells was measured after 4 h incubation in the presence of peptides in buffer (PBS, pH 7.4) supplemented with 10% standard cell culture medium to guarantee the metabolic efficacy of the cells during the incubation period.

ii) The ability of the peptides to impair the membrane integrity of adherently growing cells was investigated by the LDH assay (Fig. 4). This assay is based on the detection of the cytosolic enzyme LDH in the cell culture supernatant after an incubation period of 4 h with peptides. The LDH assay was performed in buffer (PBS, pH 7.4) as well as in Bionas running medium (BRM, pH 7.4) for a direct comparison of the LDH assay results to the on-chip measurements (see below).

iii) Furthermore, we analyzed peptide-induced membrane permeabilization of suspended cells by the uptake of the DNA-intercalating fluorescent dye PI upon the interaction with peptides in buffer for 30 min (Fig. 5).

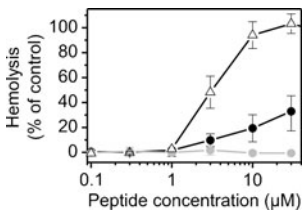

Fig. 2 Hemolytic activity of peptides. Lysis of human erythrocytes was determined photometrically by measuring the release of hemoglobin after incubation with peptides in PBS at 37 °C for 30 min. NK-2, solid black circles; NK11, solid grey circles; melittin, open triangles

Table 2 Comparison of the cytotoxicity of peptides against LA-N-1 NB and HaCaT cells using different types of endpoint tests. The peptide concentration (IC_{50}) which reduced the metabolic activity by 50% (MTT test) or which induced 50 % efflux (LDH assay) or influx (PI uptake assay) are given in μM. The LDH test was performed in buffer (PBS, pH 7.4) and in medium (BRM)

	MTT	LDH (PBS)	LDH (BRM)	PI
LA-N-1 NB cells				
NK-2	3.6±0.4	11.4±1.6	20.2±3.3	12.0±1.6
NK11	>>100	>>100	>>100	>>100
Melittin	1.2±0.1	2.1±0.6	1.9±0.4	2.8±0.3
HaCaT cells				
NK-2	7.3±0.8	10.9±0.2	31.2±5.2	26.8±0.6
NK11	>>100	>>100	>>100	>>100
Melittin	2.6±0.3	3.2±0.4	4.8±0.3	9.5±1.4

Melittin and NK-2 exhibited potent anti-cancer cell activities, whereas NK11 was completely inactive against the two cell lines. For NK-2, we determined IC_{50} values of 3.6–20.2 μM and of 7.3–31.2 μM towards LA-N-1 and HaCaT cells, respectively. Thus demonstrating a distinctive selectivity between the cell lines. Melittin exhibited a similar cell type dependency as NK-2. It was the most active peptide in this group and its activity against the NB cells was independent of the assay. Hence, the apparent cytotoxic activity of a given peptide appeared to be strongly dependent on the assay type and on the conditions the assay was performed.

Binding of NBD-labelled peptides to the cancer cells

LA-N-1 and HaCaT cells were suspended by trypsination and the binding of the fluorescently labelled peptides NBD-NK-2 and NBD-NK11 was measured by flow cytometry. As a prerequisite, we determined the effect of the NBD

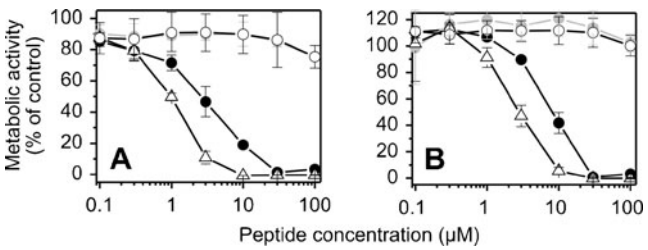

Fig. 3 Cytotoxic activity of peptides (I). Metabolic activity of (**a**) LA-N-1 NB cells and of (**b**) HaCaT keratinocytes measured by the MTT assay in PBS, pH 7.4, supplemented with 10% cell culture medium. Cells were incubated in the buffer/medium mix as a control (open circles) or with peptides (NK-2, black filled circles; NK11, grey filled circles; and melittin, open triangles) at indicated concentrations for 4 h at 37 °C

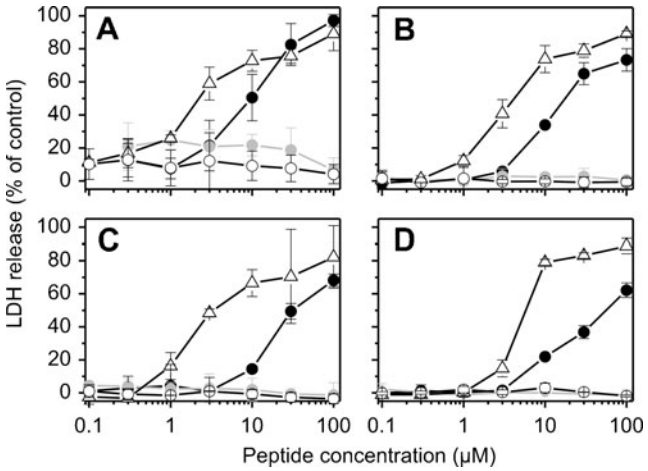

Fig. 4 Cytotoxic activity of peptides (II). Membrane damage of (**a**, **c**) LA-N-1 NB cells and (**b**, **d**) HaCaT keratinocytes measured by the release of cytosolic enzyme LDH. Cells were incubated with indicated amounts of peptides in PBS, pH 7.4 (upper panel), and in BRM (lower panel) for 4 h at 37 °C. NK-2, black filled circles; NK11, grey filled circles; melittin, open triangles; control, open circles

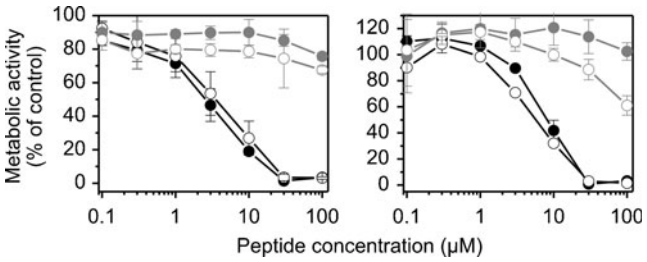

Fig. 6 Influence of the fluorescent label NBD on the cytotoxicity of peptides. Metabolic activity of (**a**) LA-N-1 NB cells and of (**b**) HaCaT keratinocytes was measured by the MTT assay. Cells were incubated with peptides (NK-2, black filled circles; NBD-NK-2, open black circles; NK11, grey filled circles; NBD-NK11; open grey circles) at indicated concentrations for 4 h at 37 °C

modification on the cytotoxicity of the peptides by the MTT test (Fig. 6): No influence of the NBD group was detectable for NK-2. For NK11, the attachment of the NBD group had a negligible effect on its cytotoxicity against LA-N-1 cells, however, cytotoxicity considerably increased against HaCaT cells (Fig. 6). The latter effect must be taken under consideration when evaluating the binding of the NBD modified peptides to the cells.

The two peptides clearly differ in their capability to bind to the cancer cells. The measured green fluorescence of the cells, as a marker of the amount of bound peptide, was considerably higher for cells incubated with NBD-NK-2 than for cells incubated with NBD-NK11 (Figs. 7 and 8). In the presence of higher concentrations of NBD-NK11, two cell populations emerge, which differ in both the amount of NBD-NK11 attached to the cells and the size of the cells (Fig. 7, panel C). The binding of the peptide was enhanced to shrinked cells, which most probably represent damaged cells. At first glance, binding of peptides appeared to be very similar for both cell types with a considerable increase of green fluorescence, reflecting peptide binding to the cells, at 10 μM peptide concentration. It should be emphasized, however, that minor binding of NBD-NK-2 to LA-N-1 cells could be detected already at 1 μM NBD-NK-2.

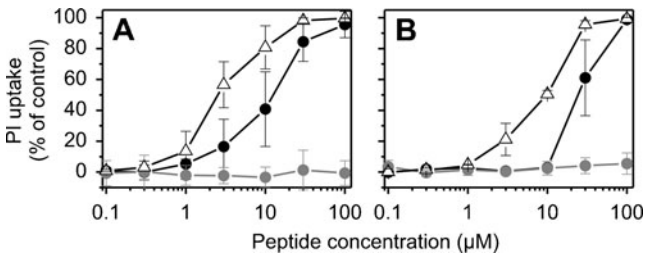

Fig. 5 Cytotoxic activity of peptides (III). Peptide-induced membrane permeabilization was detected by PI uptake by (**a**) LA-N-1 NB cells and by (**b**) HaCaT keratinocytes. Cells were incubated with peptides (NK-2, black filled circles; NK11, grey filled circles; and melittin, open triangles) in PBS, pH 7.4, for 30 min at 37 °C. Uptake of the fluorescent dye PI by membrane-compromised cells was determined by FACS analysis

Online monitoring of peptide-induced changes in cell metabolism and morphology/adhesion

The impact of various concentrations of peptides to adhesion/morphology and metabolic activity of LA-N-1 and HaCaT cells were monitored in real time and online by the use of a chip-based sensor. Cells were grown adherently on chips, which are equipped with impedance, pH and oxygen sensors (see also Fig. 9a–c). If cells on the chip were perfused with running medium, impedance and rates for cell respiration (changes in O_2 signal) and acidification (changes in pH) were more or less constant for >20 h (not shown). In the case that cells die, metabolic rates (respiration and acidification) were reduced. Moreover, impedance, i.e. the electric isolation of the chip surface by the cells, decreased if cells rounded up, lost their tight contact or got detached from the chip surface. Electrical signals obtained for impedance had always a high quality, whereas signals for pH and pO_2 were more noisy. This might explain some ups and downs in the curves. Comparable to the standard cytotoxicity tests, melittin was also most effective in the chip-based measurements. A peptide concentration of 0.3 μM was sufficient to induce killing of NB cells after perfusion for 6 h. Just before cells died, they responded to the melittin treatment by an enhanced acidification rate (i.e. glycolysis, Fig. 9c, arrows). Interestingly, the kinetics of killing after this brief stress response were very similar and rather independently of the actual melittin concentration. HaCaT cells were less sensitive than LA-N-1 cells to peptide treatment. The changes in metabolism of HaCaT cells as a response to

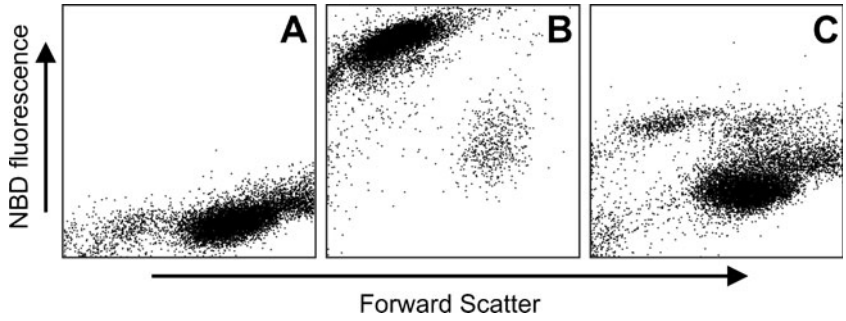

Fig. 7 Binding of NBD-labelled peptides to LA-N-1 NB cells. Cells were incubated (**a**) in buffer alone, (**b**) with 30 μM NBD-NK-2, and (**c**) with 30 μM NBD-NK11 for 30 min at 37 °C and were subsequently analysed by flow cytometry

peptides were more dramatic. Heterogeneous results were observed for 1 μM melittin, which is apparently a threshold concentration. In one set of experiments cells were initially damaged, indicated by a slight decrease in impedance, than cells recovered again (increase in impedance) while they were continuously perfused with peptide-containing medium (Fig. 9c, circle).

The selectivity of NK-2 for LA-N-1 over HaCaT cells was underlined by the chip-based measurements (Fig. 9a). Worth mentioning, both cell types responded rapidly to NK-2 treatment by an increase in impedance, which is enduring in case of sublethal concentrations of NK-2. Even for peptide NK11 we could document a significant impact on the cells (Fig. 9b), though it was absolutely non-toxic up to 100 μM in the standard assays (see above). An increase in impedance was obtained for NK11 treated LA-N-1 cells, similar to the effect observed for NK-2. The delayed increase after 13 h induced by 10 μM NK11, when compared to a faster increase after 2 h for 30 μM NK11, suggests that the peptide accumulated on the cell surface until it reached a critical concentration sufficient to induce changes in cell adhesion and/or morphology.

In addition to the on-chip electrical measurements, we monitored the appearance of the cells on the chips by light microscopy. Therefore, chips were removed from the fluidic system during the stop phase, imaged and immediately replaced. This has been done representatively for NK-2 (Fig. 10). Before the experiment, confluent cell layers were observed for both cell types. After perfusion with NK-2, LA-N-1 cells were rounded up and largely detached from the surface. The layer of HaCaT cells appeared almost unaltered by NK-2 (Fig. 10). Hence, NK-2 induced subtle morphological changes of HaCaT cells detected by impedance measurements were not visible by light microscopy at this magnification.

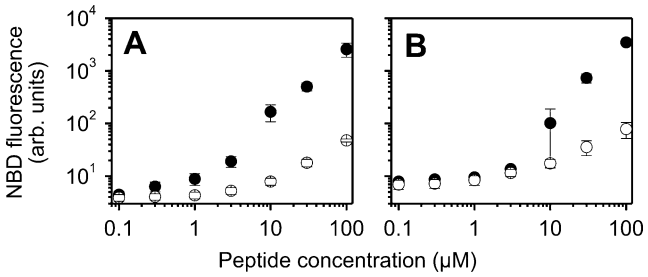

Fig. 8 Binding of NBD-labelled peptides to cells. FACS analysis of (**a**) LA-N-1 NB cells and of (**b**) HaCaT keratinocytes after incubation with indicated amounts of fluorescently-labelled peptides. NBD-NK-2, filled black circles; NBD-NK11, open circles

Discussion

The aim of this study was to establish a chip-based sensor to monitor the dynamic interplay of membrane-interacting peptides with human cells. As a proof of principle, we focussed on two established cell lines and three well-characterized peptides. As the peptides are potential lead structures for the development of anti-cancer drugs, it is of utmost important to elucidate (i) their cytotoxicity against a variety of cancer cells and normal cells, (ii) their detailed mode of action, (iii) their killing kinetics and (iv) the response of the target cells to peptide treatment. (i) Cytotoxicity screening was performed using classical endpoint tests, such as the MTT test, the LDH-release assay and the PI-uptake assay. To address points (iii) to (iv) we took advantage of cells cultivated on the chip surface of a sensor connected with a perfusion system. This setup enabled us to monitor the effects of the peptides on the metabolism and cell morphology / adhesion in real time.

The differential cytotoxicity of peptide NK-2 against human NB cancer cells and keratinocytes has been established before (Andrä and Leippe 1999; Schröder-Borm et al. 2005) and could be impressively also documented here with the Bionas analyzing system. In fact, target cell selectivity of NK-2 was even more clearly expressed compared to the endpoint tests and documented superiority of NK-2 over melittin regarding this issue. The slightly improved binding of NK-2 to NB cells might contribute to this selectivity (Fig. 8). With the classical cytotoxicity tests we observed peptide-induced cell membrane damage within 30 min, and blockage of the residual metabolic activity, thus killing of the cells, within 4 h. This killing kinetic is extremely fast compared to other chemotherapeutic drugs and will hamper the emergence of resistances against the

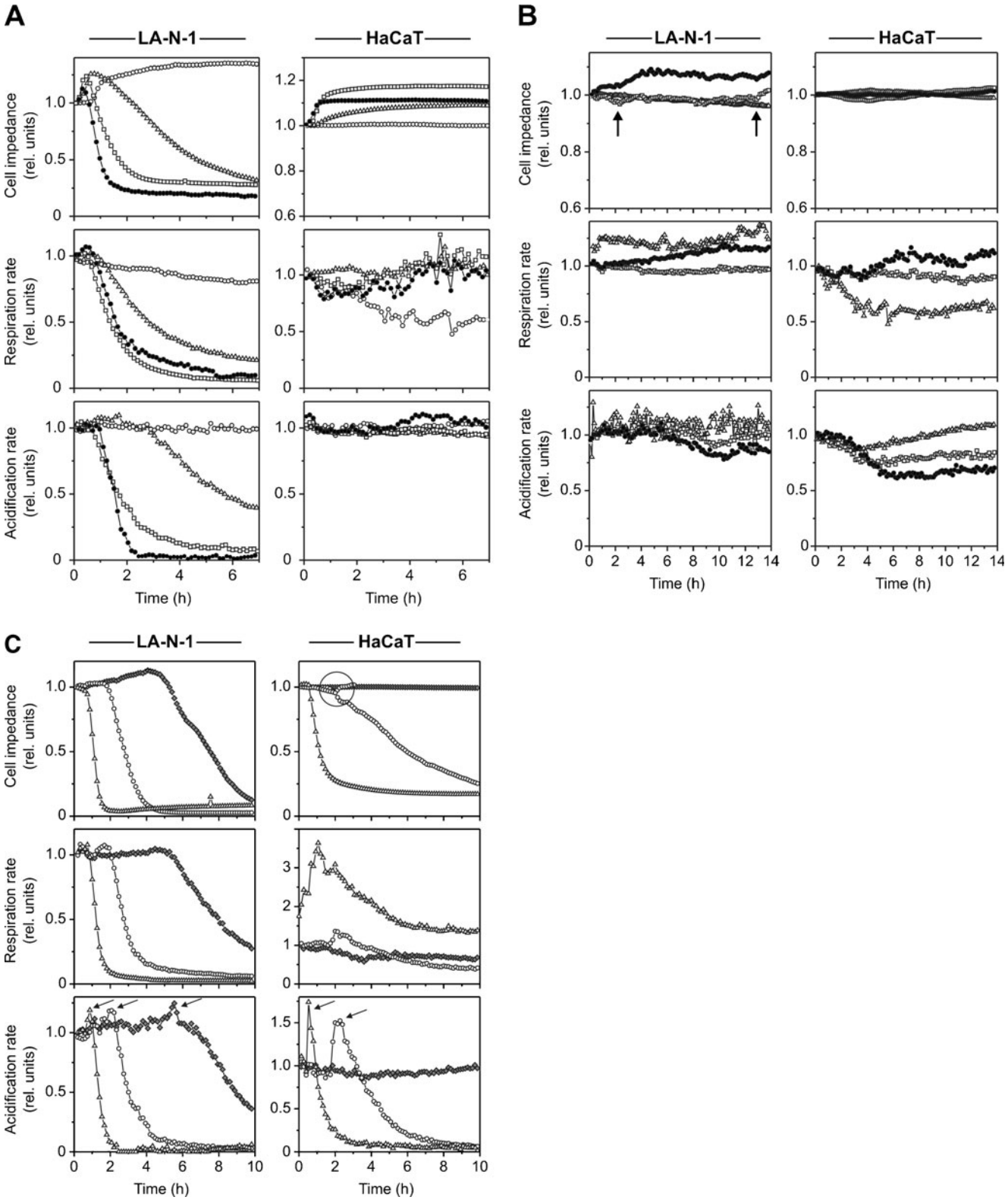

Fig. 9 Online monitoring of cell metabolism and morphology/adhesion by the use of a chip-based biosensor. Cells grown on a chip were perfused with running medium which contained various amounts of peptides (**a**) NK-2, (**b**) NK11, and (**c**) melittin; 0.3 μM (filled grey diamonds), 1 μM (open circles), 3 μM (open triangles), 10 μM (open squares), 30 μM (filled black circles). Respiration rate (oxygen consumption), and acidification rate of the medium as well as cell layer impedance are shown relative to untreated control cells. Cell impedance values of "1.0" and "0" comply with a sensor chip covered with cells, and no cells on a chip, respectively

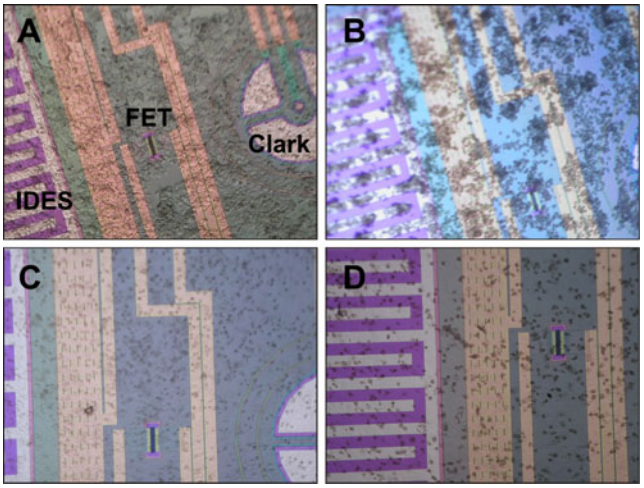

Fig. 10 Light microscopy images of cell layers on biosensor chips. Images of LA-N-1 NB cells (**a**;**b**) and of HaCaT keratinocytes (c, d) were taken before (**a**, **c**) and after perfusion with 10 μM NK-2 for 18 h (**b**) and with 30 μM NK-2 for 22 h (**d**), respectively. Sensors for pH (FET), O_2 (Clark) and interdigitated electrode structures (IDES) for the measurement of impedance are indicated in (**a**)

peptides. Moreover, the online-monitoring of the cells on the sensor chip revealed an immediate response to the peptides by morphological changes or by an modulated metabolism. Killing was completed after 1–2 h for NK-2 and melittin. Preceding the cytotoxic effects of NK-2, we observed an increase in cell impedance, which may be due a closer cell-cell contact, an increase in cell adhesion or flattening of the cell layer. This morphological effect of NK-2 was observed for both cell types and seemed to be characteristic for the action of the peptide. It was not observed for melittin indicating a different type of peptide-cell interaction. Interestingly, also NK11, the inactive variant of NK-2, led to a similar increase in impedance upon addition to LA-N-1 cells. Such an increase in impedance has been observed rarely and it has been shown that it is not associated with cell damage, or an effect on the organization of the cytoskeleton (Ceriotti et al. 2007; Thedinga et al. 2007), which led to a decrease in impedance, but with cycloheximide-mediated inhibition of protein biosynthesis in HT-29 cells (Thedinga et al. 2007), suggesting intracellular structures as secondary targets for NK-2. Among the three peptides, melittin was most effective. This confirmed the high hemolytic activity and potent killing efficacy of melittin that has been documented in many studies by us and others before and is based on its high hydrophobicity (Andrä and Leippe 1999; Blondelle and Houghten 1991; Leippe et al. 1994; Schröder-Borm et al. 2005; Werkmeister et al. 1993). It is worth to mention that cell killing by melittin was preceded by an enhanced cell metabolism, probably a stress response to the peptide-induced cell damage.

Target selectivity is an important issue and from the presented data it may be speculated, that selectivity is connected with the hydrophobicity profile and the overall hydrophobicity of the peptides. A nearly perfect amphipathic secondary structure, which can be adapted by NK-2, is the basis for selectivity.

From our data it can be concluded, that the tested peptides accumulate on the cell surface until they reach a critical concentration, which is necessary to result in cell response and/or cell damage. This critical concentration can of course also be reached for low-concentration solutions of peptides due to the fact, that the cells are continuously perfused by fresh peptide solution. The latter fact is an important difference to classical cytotoxicity tests, where a constant volume and thus a defined amount of the drug is incubated with the cells. Such an effect is nicely observed for melittin. At certain time points, LA-N-1 cells respond by a sharp and short increase in acidification rate, then the cells underwent cell death, which is evidenced by an decrease to zero for all three measuring parameters. Even NK11, which was absolutely non-cytotoxic up to 100 μM to both cell lines when analyzed with the end-point tests, induced a significant increase in impedance of LA-N-1 cells after long-term perfusion of the cells with the peptide at a tenfold reduced concentration. This characteristic of a perfusion-based analyzing system impedes the definition of a clear-cut IC_{50}, however, demonstrates on the other hand that this system monitors extremely sensitive any peptide-induced cell response. Other authors have defined a dynamic IC_{50} after a defined perfusion time. i.e. 24 h (Thedinga et al. 2007).

In conclusion, with the chip-based sensor system we were able to monitor the kinetics of killing, and could reproduce cytotoxic properties of the peptides derived from endpoint tests. IC_{50} values obtained from classical endpoint tests are not necessarily comparable to dynamic IC_{50} values, which can be derived from the measuring curves of the sensor system. However, the application of drugs to a cell layer in a discontinuous perfusion system imitates an in vivo situation much better than cytotoxicity tests in 96-well plates and is, at least in our opinion, a clear advantage of the sensor system. Moreover, we observed peptide-specific metabolic and morphological responses of the cells as well as cell recovery during treatment. Despite the fact, that both peptides, NK-2 and melittin, interact with membranes and induce membrane depolarization or lysis (Benachir and Lafleur 1995; Schröder-Borm et al. 2003), our findings suggest different modes of action, which would have been overlooked by other cytotoxicity assays.

Acknowledgements We would like to give our thanks to Sabrina Groth for excellent technical assistance in cell culture and FACS analysis. This work has been financially supported by the German Science Foundation (DFG), grant AN301/5-1.

References

Abarzua S, Drechsler S, Fischer K, Pietschmann N, Stapel J, Duda S, Richter DU, Ehret R, Piechulla B, Briese V (2010) Online monitoring of cellular metabolism in the MCF-7 carcinoma cell line treated with phytoestrogen extracts. Anticancer Res 30:1587–1592

Andjelkovic T, Pesic M, Bankovic J, Tanic N, Markovic ID, Ruzdijic S (2008) Synergistic effects of the purine analog sulfinosine and curcumin on the multidrug resistant human non-small cell lung carcinoma cell line (NCI-H460/R). Cancer Biol Ther 7:1024–1032

Andrä J, Leippe M (1999) Candidacidal activity of shortened synthetic analogs of amoebapores and NK-lysin. Med Microbiol Immunol 188:117–124

Andrä J, Koch MHJ, Bartels R, Brandenburg K (2004) Biophysical characterization of the endotoxin inactivation by NK-2, an antimicrobial peptide derived from mammalian NK-Lysin. Antimicrob Agents Chemother 48:1593–1599

Andrä J, Monreal D, Martinez de Tejada G, Olak C, Brezesinski G, Sanchez Gomez S, Goldmann T, Bartels R, Brandenburg K, Moriyon I (2007) Rationale for the design of shortened derivatives of the NK-lysin derived antimicrobial peptide NK-2 with improved activity against Gram-negative pathogens. J Biol Chem 282:14719–14728

Baker MA, Maloy WL, Zasloff M, Jacob LS (1993) Anticancer efficacy of magainin 2 and analogue peptides. Cancer Res 53:3052–3057

Bechinger B, Lohner K (2006) Detergent-like actions of linear amphipathic cationic antimicrobial peptides. Biochim Biophys Acta 1758:1529–1539

Benachir T, Lafleur M (1995) Study of vesicle leakage induced by melittin. Biochim Biophys Acta 1235:452–460

Blondelle SE, Houghten RA (1991) Hemolytic and antimicrobial activities of the twenty-four individual omission analogous of melittin. Biochemistry 30:4671–4678

Bodek G, Vierre S, Rivero-Müller A, Huhtaniemi I, Ziecik AJ, Rahman NA (2005) A novel targeted therapy of Leydig and granulosa cell tumors through the luteinizing hormone receptor using a hecate-chorionic gonatropin b conjugate in transgenic mice. Neoplasia 7:497–508

Boukamp P, Petrussevska RT, Breitkreutz D, Hornung J, Markham A, Fusenig NE (1988) Normal keratinization in a spontaneously immortalized aneuploid human keratinocyte cell line. J Cell Biol 106:761–771

Ceriotti L, Kob A, Drechsler S, Ponti J, Thedinga E, Colpo P, Ehret R, Rossi F (2007) Online monitoring of BALB/3 T3 metabolism and adhesion with multiparametric chip-based system. Anal Biochem 371:92–104

Chen YQ, Min C, Sang M, Han YY, Ma X, Xue XQ, Zhang SQ (2010) A cationic amphiphilic peptide ABP-CM4 exhibits selective cytotoxicity against leukemia cells. Peptides 31:1504–1510

Chuang CM, Monie A, Wu A, Mao CP, Hung CF (2008) Treatment with LL-37 peptide enhances the antitumor effects induced by CpG oligodeoxynucleotides against ovarian cancer. Hum Gene Ther

Cruciani RA, Barker JL, Zasloff M, Chen HC, Colamonici O (1991) Antibiotic magainins exert cytolytic activity against transformed cell lines through channel formation. Proc Natl Acad Sci USA 88:3792–3796

Dempsey CE (1990) The action of melittin on membranes. Biochim Biophys Acta 1031:143–161

Eisenberg D, Schwarz E, Komaroy M, Wall R (1984) Analysis of membrane and surface protein sequences with the hydrophobic moment plot. J Mol Biol 179:125–142

Habermann E, Jentsch J (1967) Sequenzanalyse des Melittins aus den tryptischen und peptischen Spaltstücken. Hoppe-Seyler´s Z Physiol Chem 351:884–890

Hammer M, Brauser A, Olak C, Brezesinski G, Goldmann T, Gutsmann T, Andrä J (2010) Lipopolysaccharide interaction is decisive for the activity of the antimicrobial peptide NK-2 against *Escherichia coli* and *Proteus mirabilis*. Biochem J 427:477–488

Harder J, Bartels J, Christophers E, Schröder JM (1997) A peptide antibiotic from human skin. Nature 387:861

Harder J, Bartels J, Christophers E, Schröder JM (2001) Isolation and characterization of human beta-defensin-3, a novel human inducible peptide antibiotic. J Biol Chem 276:5707–5713

Hoskin DW, Ramamoorthy A (2008) Studies on anticancer activities of antimicrobial peptides. Biochim Biophys Acta 1778:357–375

Hui L, Leung K, Chen HM (2002) The combined effects of antibacterial peptide cecropin A and anti-cancer agents on leukemia cells. Anticancer Res 22:2811–2816

Jenssen H, Hamill P, Hancock RE (2006) Peptide antimicrobial agents. Clin Microbiol Rev 19:491–511

Johnstone SA, Gelmon K, Mayer LD, Hancock RE, Bally MB (2000) In vitro characterization of the anticancer activity of membrane-active cationic peptides. I. Peptide-mediated cytotoxicity and peptide-enhanced cytotoxic activity of doxorubicin against wild-type and p-glycoprotein over-expressing tumor cell lines. Anticanc Drug Des 15:151–160

Kim S, Kim SS, Bang YJ, Kim SJ, Lee BJ (2003) In vitro activities of native and designed peptide antibiotics against drug sensitive and resistant tumor cell lines. Peptides 24:945–953

Kyte J, Doolittle RF (1982) A simple method for displaying the hydropathic character of a protein. J Mol Biol 157:105–132

Larrick JW, Hirata M, Zhong J, Wright SC (1995) Anti-microbial activity of human CAP18 peptides. Immunotechnology 1:65–72

Leippe M, Andrä J, Müller-Eberhard HJ (1994) Cytolytic and antibacterial activity of synthetic peptides derived from amoebapore, the pore-forming peptide of *Entamoeba histolytica*. Proc Natl Acad Sci USA 91:2602–2606

Makovitzki A, Fink A, Shai Y (2009) Suppression of human solid tumor growth in mice by intratumor and systemic inoculation of histidine-rich and pH-dependent host defense-like lytic peptides. Cancer Res 69:3458–3463

Matsuzaki K, Sugishita K, Fujii N, Miyajima K (1995) Molecular basis for membrane selectivity of an antimicrobial peptide, magainin 2. Biochemistry 34:3423–3429

Ohsaki Y, Gazdar AF, Chen HC, Johnson BE (1992) Antitumor activity of magainin analogues against human lung cancer cell lines. Cancer Res 52:3534–3538

Papo N, Braunstein A, Eshhar Z, Shai Y (2004) Suppression of human prostate tumor growth in mice by a cytolytic D-, L-amino Acid Peptide: membrane lysis, increased necrosis, and inhibition of prostate-specific antigen secretion. Cancer Res 64:5779–5786

Papo N, Seger D, Makovitzki A, Kalchenko V, Eshhar Z, Degani H, Shai Y (2006) Inhibition of tumor growth and elimination of multiple metastases in human prostate and breast xenografts by systemic inoculation of a host defense-like lytic peptide. Cancer Res 66:5371–5378

Russell PJ, Hewish D, Carter T, Sterling-Levis K, Ow K, Hattarki M, Doughty L, Guthrie R, Shapira D, Molloy PL, Werkmeister JA, Kortt AA (2004) Cytotoxic properties of immunoconjugates containing melittin-like peptide 101 against prostate cancer: in vitro and in vivo studies. Cancer Immunol Immunother 53:411–421

Schröder-Borm H, Willumeit R, Brandenburg K, Andrä J (2003) Molecular basis for membrane selectivity of NK-2, a potent peptide antibiotic derived from NK-lysin. Biochim Biophys Acta 1612:164–171

Schröder-Borm H, Bakalova R, Andrä J (2005) The NK-lysin derived peptide NK-2 preferentially kills cancer cells with increased surface levels of negatively charged phosphatidylserine. FEBS Lett 579:6128–6134

Schweizer F (2009) Cationic amphiphilic peptides with cancer-selective toxicity. Eur J Pharmacol 625:190–194

Stortecky S, Suter TM (2010) Insights into cardiovascular side-effects of modern anticancer therapeutics. Curr Opin Oncol 22:312–317

Tang C, Shao X, Sun B, Huang W, Qiu F, Chen Y, Shi YK, Zhang EY, Wang C, Zhao X (2010) Anticancer mechanism of peptide P18 in human leukemia K562 cells. Org Biomol Chem 8:984–987

Thedinga E, Kob A, Holst H, Keuer A, Drechsler S, Niendorf R, Baumann W, Freund I, Lehmann M, Ehret R (2007) Online monitoring of cell metabolism for studying pharmacodynamic effects. Toxicol Appl Pharmacol 220:33–44

Wang KR, Yan JX, Zhang BZ, Song JJ, Jia PF, Wang R (2009) Novel mode of action of polybia-MPI, a novel antimicrobial peptide, in multi-drug resistant leukemic cells. Cancer Lett 278:65–72

Warren P, Li L, Song W, Holle E, Wei Y, Wagner T, Yu X (2001) In vitro targeted killing of prostate tumor cells by a synthetic amoebapore helix 3 peptide modified with two gamma-linked glutamate residues at the COOH terminus. Cancer Res 61:6783–6787

Werkmeister JA, Kirkpatrick A, McKenzie JA, Rivett DE (1993) The effect of sequence variations and structure on the cytolytic activity of melittin peptides. Biochim Biophys Acta 1157:50–54

Zanetti M, Gennaro R, Romeo D (1995) Cathelicidins: a novel protein family with a common proregion and a variable C-terminal antimicrobial domain. FEBS Lett 374:1–5

Zasloff M (1987) Magainins, a class of antimicrobial peptides from *Xenopus* skin: Isolation, characterization of two active forms, and partial cDNA sequence of a precursor. Proc Natl Acad Sci USA 84:5449–5453

Zasloff M (2002) Antimicrobial peptides of multicellular organisms. Nature 415:389–395